JOURNAL OF Applied Polymer SCIENCE

Special Issue: Bio-based Packaging

Guest Editors: José M. Lagarón, Amparo López-Rubio, and María José Fabra
Institute of Agrochemistry and Food Technology of the Spanish Council for Scientific Research

EDITORIAL

REVIEWS

RESEARCH ARTICLES

JOURNAL OF Applied Polymer SCIENCE

Special Issue: Bio-based Packaging

Guest Editors: José M. Lagarón, Amparo López-Rubio, and María José Fabra
Institute of Agrochemistry and Food Technology of the Spanish Council for Scientific Research

Impact of fermentation residues on the thermal, structural, and rheological properties of polyhydroxy(butyrate-*co*-valerate) produced from cheese whey and olive oil mill wastewater
L. Hilliou, D. Machado, C. S. S. Oliveira, A. R. Gouveia, M. A. M. Reis, S. Campanari, M. Villano and M. Majone, *J. Appl. Polym. Sci.* 2015, DOI: 10.1002/app.42818

Synergistic effect of lactic acid oligomers and laminar graphene sheets on the barrier properties of polylactide nanocomposites obtained by the in situ polymerization pre-incorporation method
J. Ambrosio-Martín, A. López-Rubio, M. J. Fabra, M. A. López-Manchado, A. Sorrentino, G. Gorrasi and J. M. Lagarón, *J. Appl. Polym. Sci.* 2015, DOI: 10.1002/app.42661

Antibacterial poly(lactic acid) (PLA) films grafted with electrospun PLA/allyl isothiocyanate fibers for food packaging
H. H. Kara, F. Xiao, M. Sarker, T. Z. Jin, A. M. M. Sousa, C.-K. Liu, P. M. Tomasula and L. Liu, *J. Appl. Polym. Sci.* 2015, DOI: 10.1002/app.42475

Poly(L-lactide)/ZnO nanocomposites as efficient UV-shielding coatings for packaging applications
E. Lizundia, L. Ruiz-Rubio, J. L. Vilas and L. M. León, *J. Appl. Polym. Sci.* 2015, DOI: 10.1002/app.42426

Effect of electron beam irradiation on the properties of polylactic acid/montmorillonite nanocomposites for food packaging applications
M. Salvatore, A. Marra, D. Duraccio, S. Shayanfar, S. D. Pillai, S. Cimmino and C. Silvestre, *J. Appl. Polym. Sci.* 2015, DOI: 10.1002/app.42219

Preparation and characterization of linear and star-shaped poly L-lactide blends
M. B. Khajeheian and A. Rosling, *J. Appl. Polym. Sci.* 2015, DOI: 10.1002/app.42231

Mechanical properties of biodegradable polylactide/poly(ether-block-amide)/thermoplastic starch blends: Effect of the crosslinking of starch
L. Zhou, G. Zhao and W. Jiang, *J. Appl. Polym. Sci.* 2015, DOI: 10.1002/app.42297

Interaction and quantification of thymol in active PLA-based materials containing natural fibers
I. S. M. A. Tawakkal, M. J. Cran and S. W. Bigger, *J. Appl. Polym. Sci.* 2015, DOI: 10.1002/app.42160

Graphene-modified poly(lactic acid) for packaging: Material formulation, processing, and performance
M. Barletta, M. Puopolo, V. Tagliaferri and S. Vesco, *J. Appl. Polym. Sci.* 2015, DOI: 10.1002/app.42252

Edible films based on chia flour: Development and characterization
M. Dick, C. H. Pagno, T. M. H. Costa, A. Gomaa, M. Subirade, A. De O. Rios and S. H. Flóres, *J. Appl. Polym. Sci.* 2015, DOI: 10.1002/app.42455

Influence of citric acid on the properties and stability of starch-polycaprolactone based films
R. Ortega-Toro, S. Collazo-Bigliardi, P. Talens and A. Chiralt, *J. Appl. Polym. Sci.* 2015, DOI: 10.1002/app.42220

Bionanocomposites based on polysaccharides and fibrous clays for packaging applications
A. C. S. Alcântara, M. Darder, P. Aranda, A. Ayral and E. Ruiz-Hitzky, *J. Appl. Polym. Sci.* 2015, DOI: 10.1002/app.42362

Hybrid carrageenan-based formulations for edible film preparation: Benchmarking with kappa carrageenan
F. D. S. Larotonda, M. D. Torres, M. P. Gonçalves, A. M. Sereno and L. Hilliou, *J. Appl. Polym. Sci.* 2015, DOI: 10.1002/app.42263

JOURNAL OF Applied Polymer SCIENCE

Special Issue: Bio-based Packaging

Guest Editors: José M. Lagarón, Amparo López-Rubio, and María José Fabra
Institute of Agrochemistry and Food Technology of the Spanish Council for Scientific Research

Structural and mechanical properties of clay nanocomposite foams based on cellulose for the food packaging industry
S. Ahmadzadeh, J. Keramat, A. Nasirpour, N. Hamdami, T. Behzad, L. Aranda, M. Vilasi and S. Desobry, *J. Appl. Polym. Sci.* 2015, DOI: 10.1002/app.42079

Mechanically strong nanocomposite films based on highly filled carboxymethyl cellulose with graphene oxide
M. El Achaby, N. El Miri, A. Snik, M. Zahouily, K. Abdelouahdi, A. Fihri, A. Barakat and A. Solhy, *J. Appl. Polym. Sci.* 2015, DOI: 10.1002/app.42356

Production and characterization of microfibrillated cellulose-reinforced thermoplastic starch composites
L. Lendvai, J. Karger-Kocsis, Á. Kmetty and S. X. Drakopoulos, *J. Appl. Polym. Sci.* 2015, DOI: 10.1002/app.42397

Development of bioplastics based on agricultural side-stream products: Film extrusion of *Crambe abyssinica*/wheat gluten blends for packaging purposes
H. Rasel, T. Johansson, M. Gällstedt, W. Newson, E. Johansson and M. Hedenqvist, *J. Appl. Polym. Sci.* 2015, DOI: 10.1002/app.42442

Influence of plasticizers on the mechanical and barrier properties of cast biopolymer films
V. Jost and C. Stramm, *J. Appl. Polym. Sci.* 2015, DOI: 10.1002/app.42513

The effect of oxidized ferulic acid on physicochemical properties of bitter vetch (*Vicia ervilia*) protein-based films
A. Arabestani, M. Kadivar, M. Shahedi, S. A. H. Goli and R. Porta, *J. Appl. Polym. Sci.* 2015, DOI: 10.1002/app.42894

Effect of hydrochloric acid on the properties of biodegradable packaging materials of carboxymethylcellulose/poly(vinyl alcohol) blends
M. D. H. Rashid, M. D. S. Rahaman, S. E. Kabir and M. A. Khan, *J. Appl. Polym. Sci.* 2015, DOI: 10.1002/app.42870

Journal of Applied Polymer Science

Production of bacterial nanobiocomposites of polyhydroxyalkanoates derived from waste and bacterial nanocellulose by the electrospinning enabling melt compounding method

Marta Martínez-Sanz,[1] Amparo Lopez-Rubio,[1] Marianna Villano,[2] Catarina S. S. Oliveira,[3] Mauro Majone,[2] Maria Reis,[3] Jose M. Lagarón[1]

[1]Novel Materials and Nanotechnology Group, IATA, CSIC, Avda. Agustín Escardino, 7, 46980 Paterna, Valencia, Spain
[2]Department of Chemistry, Sapienza University of Rome, P.le Aldo Moro 5, 00185 Rome, Italy
[3]REQUIMTE/CQFB, FCT/Universidade Nova de Lisboa, Campus de Caparica, 2829-516 Caparica, Portugal
Correspondence to: J. M. Lagaron (E-mail: lagaron@iata.csic.es)

ABSTRACT: This work reports on the characterization of nanocomposites fully synthesized by bacteria, consisting of polyhydroxybutyrate-co-hydroxyvalerate (PHBV) matrices reinforced with bacterial cellulose nanowhiskers (BCNW). Two PHBV grades, with 9% HV (PHBV9) and 16% HV (PHBV16), were synthesized using food industry waste feedstocks and compared with a 3% HV commercial grade (PHBV3). Whereas PHBV3 presented a high barrier performance but excessive brittleness, PHBV9 and PHBV16 showed a more ductile behavior and reduced barrier properties. Subsequently, BCNW were incorporated into the PHBVs by a high-throughput electrospinning technique to produce master-batch formulations with relatively high nanofiller concentrations. The hybrid ultrathin fibers showed homogeneous morphologies and greater thermal stability than the pure PHBV fibers. Nanocomposites were then produced by melt mixing PHBVs with the hybrid fibers. Despite the low compatibility between the extremely hydrophilic BCNW and the hydrophobic PHBVs, the nanofiller was highly dispersed and provided a reduction in oxygen permeability of the PHBV3 matrix without relevant modifications in mechanical performance. © 2015 Wiley Periodicals, Inc. J. Appl. Polym. Sci. **2016**, *133*, 42486.

KEYWORDS: biopolymers and renewable polymers; cellulose and other wood products; composites

Received 20 February 2015; accepted 11 May 2015
DOI: 10.1002/app.42486

INTRODUCTION

Polyhydroxyalkanoates (PHAs) are a family of biopolyesters produced by a wide variety of bacteria as carbon storage materials.[1] These materials present a relatively wide range of properties depending on the hydroxyvalerate (HV)-to-hydroxybutyrate (HB) ratio. The highly crystalline homopolymer poly(3-hydroxybutyrate) (PHB)[2] possesses high barrier and mechanical performance, but its excessive brittleness and low thermal stability have limited its applicability within the food packaging sector. This issue may be limited by increasing the HV content up to 40–50 mol %, due to the decreased crystallinity of the so-obtained copolymers.[3–7] While this is beneficial from a manufacturing perspective, the increased amorphous character of certain PHBV grades gives rise to reduced barrier performance, limiting the potential of these materials to replace the benchmark polyethylene terephthalate polymer.[8]

The high operational costs associated to the production of PHAs[9] are one of the main constraints with regards to extending their use as food packaging materials. In this context, the use of mixed microbial cultures presents an interesting alternative versus the traditional synthesis route using pure microbial cultures, since it allows increasing the production volumes while using cheaper feedstocks. This alternative approach involves the selection of microorganisms based on their capacity for PHA storage through the application of alternate carbon substrate availability conditions.[10] As a result, large-scale fermentations may be produced without the need for sterile conditions. Furthermore, the adaptation ability of the selected microorganisms enables the use of cheap mixed substrates based on agro-food industry wastes or by-products. In addition, it has been recently demonstrated that PHAs with variable compositions and properties can be synthesized by using feedstocks with different compositions or by mixing several fermented substrates.[11]

In this work, two different PHBV grades were synthesized by mixed microbial cultures using cheese whey and olive oil mill wastewaters as substrates. These materials were characterized and compared to a commercial PHBV. To tune the properties of PHBVs, with special focus on their barrier performance,

bacterial cellulose nanowhiskers (BCNW) were incorporated as nanofillers, thus producing bionanocomposites fully synthesized by bacteria. The incorporation of plant-derived CNW has been reported in literature[12–14] and the mechanical properties of the base PHBV matrices have been seen to improve with the nanofiller addition.[12,15] However, their effect on the barrier properties was not investigated. In a recent work, we reported that the incorporation of low loadings of BCNW into PHBV matrices resulted in decreased oxygen permeability, especially at low relative humidity conditions.[16] Nevertheless, the solution casting method utilized to produce the nanocomposite films is not feasible from an industrial perspective. Attempts to prepare PHBV nanocomposites loaded with CNW by more industrially meaningful melt compounding techniques have resulted in high levels of nanofiller agglomeration[15] due to the inherent dispersion difficulties associated with this approach together with the low compatibility between the highly hydrophilic CNW and the hydrophobic PHBV. A recent work described a new method consisting of the production of master-batches by freeze-drying aqueous dispersions of PHBV and nanofibrillated cellulose (NFC).[17] Although the addition of NFC increased the tensile modulus of PHBV, thermal degradation of PHBV was seen to occur during processing and the effect on the barrier properties was not reported.

Based on our preliminary results indicating the potential of BCNW to improve the barrier of PHBV matrices,[16] the aim of this work was to improve the dispersion of BCNW in PHBV matrices by applying an innovative methodology based on the pre-incorporation of the nanofiller by electrospinning into a solid master-batch followed by the melt compounding step, which we term as electrospinning enabling melt compounding route. This procedure has been successfully used to incorporate highly dispersed BCNW into polymeric matrices such as EVOH[18,19] and PLA[20]; however, its efficiency with PHA materials has not been assessed before. The optimization of the electrospun hybrid fibers as well as the characterization of the melt processed PHBV–BCNW nanocomposites are first reported on this study.

MATERIALS AND METHODS

Materials

Three different bacterial poly(3-hydroxybutyrate-co-3-hydroxyvalerate) copolymer (PHBV) grades, with different hydroxyvalerate (HV) contents, were used throughout this study. A commercial grade with 3 mol % hydroxyvalerate (PHBV3), ENMAT Y1000P, was purchased from TianAn Biologic Materials Co. (China). PHBV grades with 16 mol % hydroxyvalerate (PHBV16) and 9 mol % hydroxyvalerate (PHBV9) were produced by mixed microbial cultures using cheese whey feedstock and olive oil mill wastewater after phenolic extraction, respectively. Bacterial cellulose (BC) mats were obtained as described in a previous work[21] and BCNW were subsequently extracted by applying the optimized method reported elsewhere.[22]

Sulphuric acid 96%, methanol, and chloroform were purchased from Panreac (Barcelona, Spain). 2,2,2-Trifluoroethanol (TFE) and polyethylene glycol 900 (PEG) were purchased from Fluka (Germany).

Synthesis of PHBVs

For the production of PHBV16, one fed-batch test was carried out in a 5 L reactor (BioStat® B plus, Sartorius) in order to produce a poly(3-hydroxybutyrate-co-3-hydroxyvalerate) copolymer using a mixed microbial culture enriched in PHA-accumulating microorganisms fed with fermented cheese whey. Due to the impossibility of producing large amounts of real fermented cheese whey, the mixed microbial culture was selected with a synthetic VFA mixture, mimicking the fermented cheese whey (% Cmol basis: 65 acetate, 15 propionate, 15 butyrate, and 5 valerate) in a 20 L sequencing batch reactor (SBR) supplemented with nutrients (NH_4Cl and KH_2PO_4, at a ratio C/N/P of 100/10/1), an organic loading rate (OLR) of 60 Cmmol L^{-1} d^{-1}, hydraulic retention time (HRT) of 1 d, sludge retention time (SRT) of 4 d, and operated at 12 h cycles with four discrete phases: influent filling (5 min); aeration (675 min); settling (30 min); and withdrawal of the exhausted effluent (10 min). The PHA production fed-batch reactor was inoculated with 2.5 L concentrated SBR mixed liquor (12.1 g VSS L^{-1}) and pulse fed with real fermented cheese whey (360 Cmmol L^{-1}), obtained from a 10 L anaerobic membrane bioreactor fed with real cheese whey. Fermented cheese whey pH was adjusted to 7.5 with the addition of 5 M NaOH, and no nutrients were supplied in order to maximize the PHA storage response. The PHA accumulation experiments were carried by feeding the fermented cheese whey pulse wise (50 Cmmol L^{-1}), controlled by dissolved oxygen response. A PHA cell content of 40 wt % was attained after *ca* 11 h. In order to recover the polymer, a quenching step (by adding 2 M HCl) was performed directly on the mixed liquor, followed by a 3 h reaction with NaClO (1% Cl_2) in order to degrade the cellular material, then the polymeric material was recovered by centrifugation (20 min × 6500 rpm), washed once with distilled water, and lyophilized for 72 h.

The PHBV9 was produced through a continuous lab-scale process consisting of an SBR and a PHA-accumulating reactor, both fed with olive oil mill wastewaters (OMWs). Prior to being used for PHA production, the OMWs were dephenolized and fermented into VFAs, as described elsewhere.[22] The SBR (1 L working volume) was inoculated with an activated sludge from the "Roma Nord" (Italy) full-scale municipal treatment plant and was operated under "feast and famine" conditions to select mixed microbial cultures with high storage ability. Based on a previous research employing a synthetic mixture of VFAs as the feedstock,[23] the length of the SBR cycle was set at 6 h, with each cycle consisting of an initial feed phase (10 min), a reaction phase (338 min), a withdrawal phase of the mixed liquor (2 min), and a regeneration phase (10 min). No settling phase was performed and, consequently, the SRT was the same as the HRT (1 day). The pH was controlled at approximately 7.5 by carbon dioxide bubbling through a compressed gas cylinder. The reactor was operated at OLR ranging from 4.74 to 8.42 g COD L^{-1} d^{-1}, obtained by diluting the fermented OMW with mineral medium containing all the nutrients needed for microbial growth. The sludge withdrawn from the SBR was directly sent to the accumulation reactor (0.35 L working volume), which was operated under nitrogen limiting conditions

(i.e., with no additional N to that contained in the OMW) and a pulse feeding strategy, consisting of four or five feeding pulses of undiluted OMW over a 6 h period. After 6 h of accumulation, the PHA-rich biomass (with a polymer content up to around 36 wt %) was recovered by means of a centrifugation step (8000 rpm, 20 min) followed by a continuous mixing with sodium hypochlorite (5% Cl_2) for several hours. The mixture was then centrifuged, washed with distilled water, and lyophilized for 96 h.

While the commercial PHBV3 grade presented a high degree of purity (>90%), the synthesized PHBV16 and PHBV9 presented a purity of *ca* 70 and 68%, respectively. To remove the impurities and avoid thermal degradation during melt processing, both PHBV grades were subjected to a purification process. Briefly, the material was dissolved in chloroform (3% w/v) at 60°C. After that, the solution was precipitated by adding it drop by drop to 10-fold excess ice-cold methanol under stirring. The precipitated fraction was separated by vacuum filtration using a Whatman filter grade 6. The solid fraction was then dried at 60°C overnight. After this purification, the materials did not seem to undergo thermal degradation, as assessed by FTIR of the polymers after being heated up to their melting temperatures for 5 min.

Characterization of the Different PHBV Grades

The concentration and composition of the synthesized PHBV grades were determined by gas chromatography (GC) after extraction, hydrolysis, and esterification to the corresponding 3-hydroxyacyl methyl esters, as described elsewhere.[24,25] Hydroxybutyrate (HB) and hydroxyvalerate (HV) concentrations were determined through the use of two calibration curves, one for HB and the other for HV, using standards (0.1–10 g L^{-1}) of a commercial PHBV (88% HB/12% HV) (Sigma), and corrected using heptadecane or benzoic acid as internal standards (concentration of approximately 1 g L^{-1}).

To determine the molecular weight of PHBV3 and PHBV16, the polymer powder was dissolved in chloroform (2 wt % concentration) at 37°C for at least 2 days. The solution was then filtered to remove all nondissolved material, and the filtrate was used to fill glass Petri dishes. Finally, chloroform was evaporated, allowing polymer recovery in the form of a thin film. These PHBV films were then characterized. Average molecular weights were determined using gel permeation chromatography as described elsewhere.[4,24]

Electrospinning

Electrospun fibers were generated from pure PHBV and PHBV–BCNW solutions in TFE. Those solutions contained a total solids content of 6 wt % and in the case of hybrid fibers, the BCNW concentration was 15% (w/w) BCNW, regarding the PHBV weight. BCNW, in the form of a partially hydrated precipitate, were dispersed in the solvent by applying intense homogenization (Ultra-turrax) for 2 min and were then stirred with the PHBV at 60°C.

A high-throughput electrospinning apparatus, the Fluidnatek® LE-500 tool of BioInicia S.L., Valencia (Spain) was used. A 40 kV voltage differential was set between the multinozzle injector and the collector and the distance between the injector and the plate was set at 10 cm. The experiments were carried out at ambient conditions.

Film Preparation

Nanocomposite PHBV films were prepared using two different methods. The traditional method of melt mixing the matrix directly with the freeze-dried nanofiller, and by melt compounding of PHBV with master-batches consisting of electrospun hybrid fibers containing 15 wt % BCNW.

For the PHBV3 matrix, both electrospun PHBV3–BCNW fibers (ES) and freeze-dried BCNW (FD) were melt mixed with the required amount of pure PHBV3 pellets to obtain blends having a final concentration of 1 and 3 wt % BCNW (sample codes: PHBV3 + 1% BCNW ES, PHBV3 + 3% BCNW ES, PHBV3 + 1% BCNW FD and PHBV3 + 3% BCNW FD). Additionally, PHBV3 was plasticized by incorporating 5 wt % PEG and samples with 1 and 3 wt % BCNW were produced by melt blending with electrospun PHBV3–BCNW fibers (sample codes: PHBV3–PEG + 1% BCNW ES and PHBV3–PEG + 3% BCNW ES).

In the case of PHBV9 and PHBV16, films containing 1 wt % BCNW, which was the optimum nanofiller loading in terms of barrier properties according to a previous study,[15] were prepared by melt mixing PHBV9–BCNW or PHBV16–BCNW fibers with the required amount of pure PHBV9 and PHBV16, respectively (sample codes: PHBV9 + 1% BCNW ES and PHBV16 + 1% BCNW ES).

PHBV blends were prepared in a Brabender Plastograph mixer for 4 min at 60 rpm and 180°C for PHBV3, 175°C for PHBV3–PEG, 155°C for PHBV9, and 140°C for PHBV16. The batches were then subjected to a rapid cooling down and they were subsequently compression molded into films using a hot-plate hydraulic press (180–140°C and 2 MPa for 2 min). The so-obtained films had a thickness between 60 and 115 μm as measured with a Mitutoyo micrometer by averaging four measurements on each sample.

Scanning Electron Microscopy (SEM)

SEM was conducted on a Hitachi microscope (Hitachi S-4100) at an accelerating voltage of 10 KV and a working distance of 12–16 mm. PHBV and PHBV–BCNW films cryofractured after immersion in liquid nitrogen were sputtered with a gold–palladium mixture under vacuum before their morphology was examined using SEM.

Differential Scanning Calorimetry (DSC)

Differential scanning calorimetry (DSC) of PHBV nanocomposites was performed on a Perkin-Elmer DSC 7 thermal analysis system using N_2 as the purging gas. The sample treatment consisted of a first heating step from −30 to 200°C, a subsequent cooling down to −30°C and a second heating step up to 200°C. The heating and cooling rates for the runs were 10°C/min and the typical sample weight was 4 mg. The first and second melting endotherms, after controlled crystallization at 10°C/min from the melt, were analyzed. Before evaluation, similar runs of an empty pan were subtracted from the DSC curves. The DSC equipment was calibrated using indium as a standard.

Table I. PHBVs Degree of Purity, Hydroxyvalerate (HV) Content, Weight-Average Molecular Weight (M_w), and Polydispersity Index (PD)

	PHBV purity (wt %)	HV (mol %)	M_w (g/mol)	PD
PHBV3	>90	3	3.8×10^5	1.6
PHBV9	68	9	1.9×10^6	1.1
PHBV16	70	16	3.6×10^5	1.7

Thermogravimetric Analysis (TGA)

Thermogravimetric (TG) curves were recorded with a TA Instruments model Q500 TGA. The samples (*ca* 20 mg) were heated from 30 to 600°C with a heating rate of 10°C/min under nitrogen atmosphere. Derivative TG curves (DTG) express the weight loss rate as a function of temperature.

Water Vapor Permeability (WVP)

Direct permeability to water was determined following a procedure similar to that described in a previous work.[16] To create a relative humidity gradient of 0–85% RH, the permeability cells were filled in with silica gel and placed inside a cabinet at 24°C and 85% RH. The solvent weight gain through a film area of 0.001 m^2 was monitored and plotted as a function of time and the permeability values were determined from the steady-state slopes obtained by doing the regression analysis of the weight gain versus time plots. The tests were done, at least, in duplicate.

Oxygen Permeability

The oxygen permeability coefficient was derived from oxygen transmission rate (OTR) measurements recorded using an Oxtran 100 equipment (Modern Control Inc., Minneapolis, MN, US), as described elsewhere.[16] Experiments were carried out at 24°C and 80% RH. Relative humidity of 80% was generated by a built-in gas bubbler and was checked with a hygrometer placed at the exit of the detector.

Mechanical Properties

Tensile tests were carried out at ambient conditions typically at 24°C and 50% RH on an Instron 4400 Universal Tester. Preconditioned dumb-bell-shaped specimens with initial gauge length of 25 mm and width of 5 mm were die-stamped from the films in the machine direction according to the ASTM D638. A fixed crosshead rate of 10 mm/min was utilized in all cases and results were taken as the average of, at least, four tests.

Statistical Analysis

One-way analysis of the variance (ANOVA) was performed using Statgraphics 5.1 software package. Comparisons between samples were evaluated using the Turkey test.

RESULTS AND DISCUSSION

Characterization of Different PHBV Grades

The main objective of this work was to produce bionanocomposite materials fully synthesized by bacteria based on PHBV matrices and using BCNW as nanofillers. Three different PHBVs were used, i.e., two grades synthesized by microbial mixed cultures using food industry waste as feedstock (PHBV9 and PHBV16) and a commercial grade (PHBV3). The degree of purity and molecular weight of these materials are gathered in Table I. As observed, the PHBV9 possessed significantly higher molecular weight and narrower polydispersity index than the other two grades. The molecular weight was not related to the valerate content, but it seemed to be conditioned by the different synthesis procedures carried out for each material. Molecular weights reported for PHBVs with similar hydroxyvalerate ratios also differ significantly depending on the culture conditions. For PHBV10 and PHBV17 produced by using pure microbial cultures of *Azotobacter chroococcum*, molecular weights of 1.5×10^6 and 1.2×10^6 g/mol, respectively, have been reported,[26] while PHBV10 and PHBV18 synthesized from microbial cultures of *Ralstonia eutropha* presented molecular weights of 6.7×10^5 and 5.6×10^5 g/mol, respectively.[27] Thus, it is clear that the culture conditions are critical in determining the molecular weight of the synthesized PHBVs. It should be noted that the synthesized grades presented lower purity than the commercial one and, therefore, an additional purification step was required in order to avoid thermal degradation during melt processing caused by the impurities remaining in the material. Previous experiments suggested that the molecular weight of PHBVs increased after the purification process, hence the purified PHBV9 and PHBV16 may present higher molecular weights than those reported in Table I.

Characterization of PHBV–BCNW Electrospun Fibers

The nanofiller incorporated into these matrices consisted of high aspect ratio (*ca* 30), highly crystalline (*ca* 95% crystallinity index), thermally stable (degradation temperature of *ca* 317°C) BCNW produced by sulphuric acid hydrolysis of bacterial cellulose pellicles.[22] To incorporate BCNW into the PHBV matrices ensuring a high dispersion, a procedure consisting on the preincorporation of BCNW into electrospun PHBV fibers, followed by the melt-mixing step, was applied and compared to the conventional method of melt mixing the polymeric matrix with freeze-dried BCNW. Regarding the preincorporation step, no previous works have reported on the production of PHBV electrospun fibers containing BCNW. Thus, in the first stage, the production of hybrid fibers by electrospinning was optimized in terms of BCNW dispersion and loading.

Although chloroform is usually chosen as solvent for the production of PHBV electrospun fibers,[28,29] it was not suitable in this case due to its incompatibility with BCNW. TFE was chosen instead, as it was expected to be compatible with both the matrix and the filler. Smooth PHBV fibers were attained for the three PHBV matrices (cf. Figure 1), in contrast with the highly porous surface characteristic from the fibers produced by using chloroform.[30] A total solids concentration of 6 wt % was selected as optimum in terms of uniform fibers morphology for the different PHBV grades. Keeping constant the solids content, BCNW were incorporated into the fibers, achieving a maximum loading of 15 wt % BCNW. As observed in Figure 1, homogeneous fibers without beads were obtained for all the systems and markedly reduced fiber diameters were attained with the addition of BCNW.

The size distributions of fibers' diameters are displayed in Figure 2. As it can be observed, PHBV9 fibers presented thicker

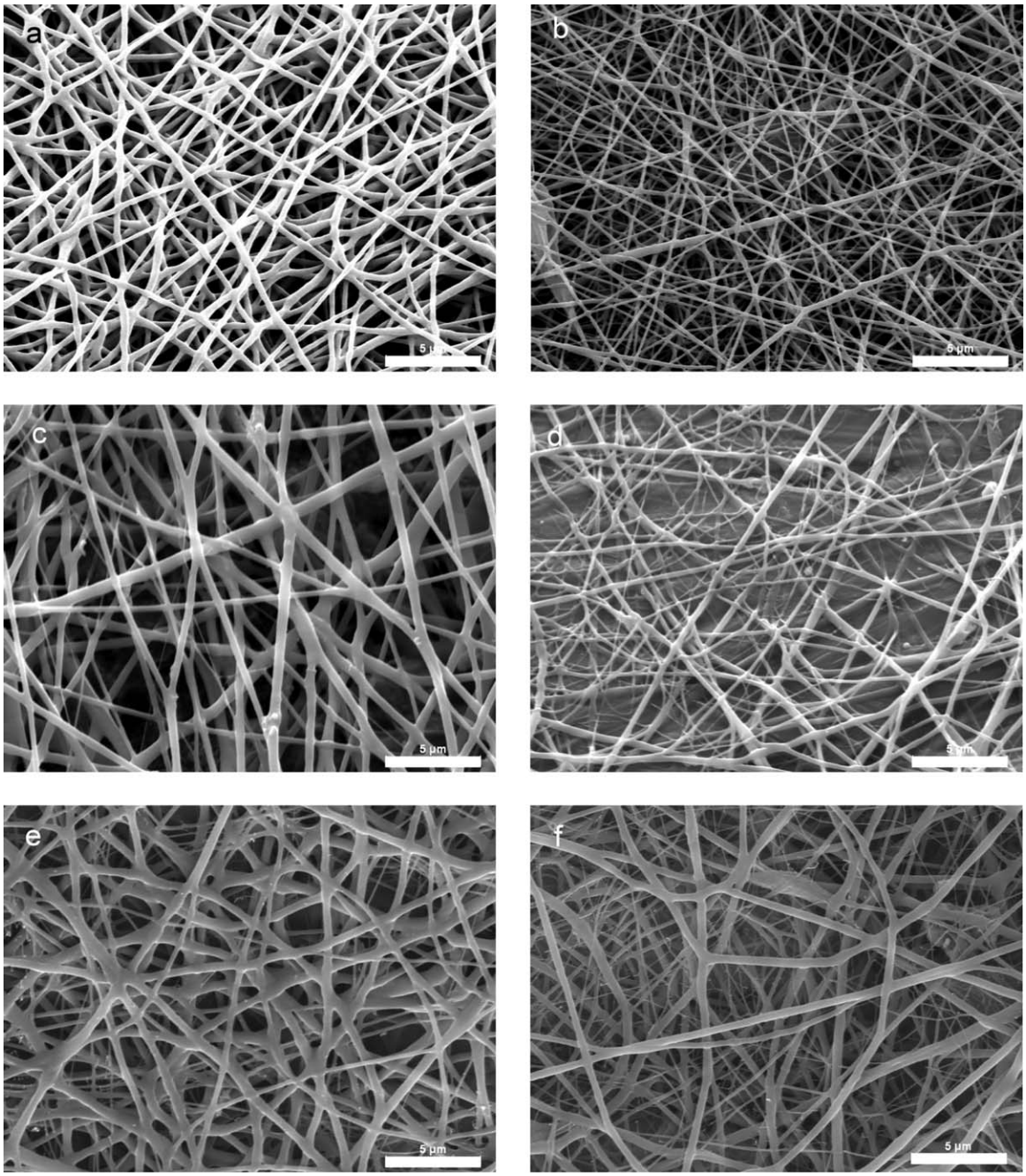

Figure 1. SEM micrographs of electrospun fibers produced from 6 wt % solutions in TFE: (a) PHBV3; (b) PHBV3 + 15% BCNW; (c) PHBV9; (d) PHBV9 + 15% BCNW; (e) PHBV16; and (f) PHBV16 + 15% BCNW. Scale markers correspond to 5 μm.

diameters than PHBV3 and PHBV16, which was probably related to the higher molecular weight and presumably higher solution viscosity of the PHBV9. Interestingly, besides reducing the average fiber diameter, the incorporation of BCNW resulted in narrower and more homogeneous size distributions. This observation has been previously reported for EVOH and PLA fibers[21,31] and it was related to the increased conductivity of solutions induced by the incorporation of BCNW. Indeed, characterization of PHBV3 solutions revealed that the viscosity increased from 482 cP to more than 2000 cP and the conductivity increased from 17 to 113 μS when incorporating 15 wt % BCNW. Although an increased viscosity usually favors the production of thicker fibers, it seems that in this case, the effect of the increased conductivity prevailed, being responsible for the diameter reduction.

The dispersion of BCNW within the fibers was assessed by TEM and Figure 3 shows a representative picture of the PHBV3 fibers containing 15 wt % BCNW. It was confirmed that BCNW were in general highly dispersed and distributed within the fibers and they were mostly stretched and aligned along the fibers longitudinal axis due to the extensional forces generated

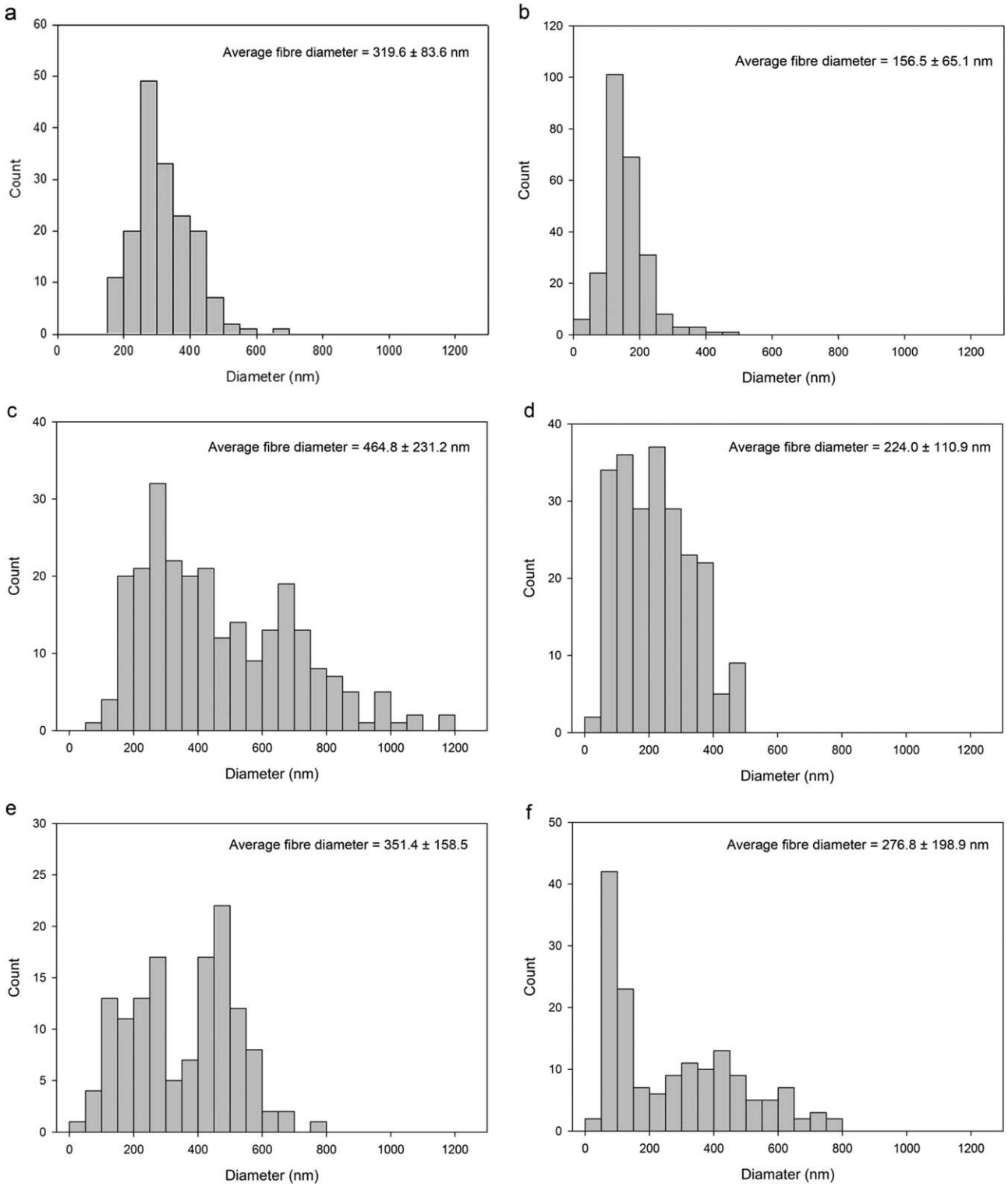

Figure 2. Histograms (taken from at least 200 measurements) representing the size distribution of electrospun PHBV and PHBV–BCNW fibers obtained from solutions containing (a) PHBV3; (b) PHBV3 + 15% BCNW; (c) PHBV9; (d) PHBV9 + 15% BCNW; (e) PHBV16; and (f) PHBV16 + 15% BCNW.

during the electrospinning process, although a few areas where BCNW were entangled could also be observed.

Thermal properties of the electrospun fibers were evaluated by DSC and TGA analyses. From the DSC results listed in Table II, it can be observed that when increasing the hydroxyvalerate content, the PHBV fibers presented lower melting temperature (T_m) and enthalpy (ΔH_m). Although the crystallinity of the samples could not be estimated since the enthalpies of the perfect PHBV crystals were not available for these particular

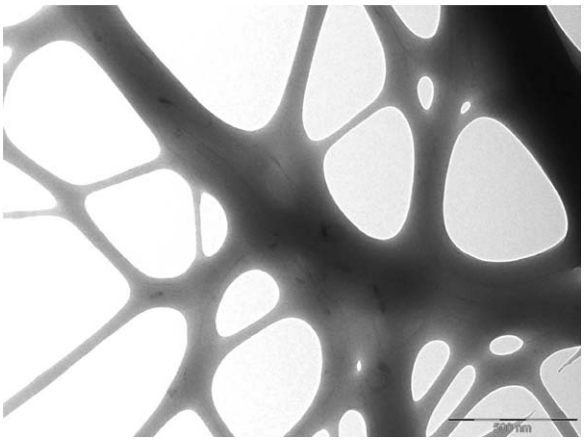

Figure 3. TEM micrograph of electrospun fibers produced from 6 wt % solutions in TFE: PHBV3 + 15% BCNW. Scale marker corresponds to 500 nm.

valerate contents, it is known that increasing the valerate ratio up to a certain point inhibits the crystallization process.[16,32,33]

In general, the incorporation of BCNW into the fibers led to lower melting temperatures, without significantly affecting the melting enthalpy and glass transition temperature. The effect of BCNW on the thermal properties of electrospun hybrid fibers has been shown to be different depending on the characteristics of the base polymer.[21,31,34,35] Thus, for high-molecular-weight PLA ($M_w = 1.5 \times 10^5$ g/mol), the incorporation of BCNW reduced the crystallinity of the fibers,[31] while the opposite effect was observed for EVOH and low-molecular-weight PLA ($M_w = 6.6 \times 10^4$ g/mol).[21,34] It seems that for the high-molecular-weight PHBVs used in this work, BCNW hindered the crystallization process to a certain extent, promoting the formation of smaller or more defective crystals, as suggested by the lower melting temperatures.

TGA analyses were carried out to evaluate the thermal stability of the electrospun fibers and to guarantee their processing at the target melt compounding temperatures without thermal degradation. The main parameters estimated from TGA curves are summarized in Table III. Increasing the hydroxyvalerate content led to slightly higher thermal stability of the PHBV fibers, as suggested by the higher onset and degradation temperatures. Furthermore, the incorporation of BCNW into the fibers gave rise to more thermally stable fibers. This effect has been previously attributed to the development of a strong intramolecular network held by PHBV–CNW hydrogen bonds.[14] It is also worth noting that while the degradation profile of the pure PHBV fibers consisted of one degradation step, the hybrid fibers showed a degradation profile composed of one major degradation peak corresponding to the PHBV followed by a second peak which accounted for approximately 15% of the total weight loss. According to the degradation temperatures reported for BCNW, i.e., 315–325°C,[22] this second peak may be assigned to the degradation of the nanofiller.

Table II. DSC Maximum of Melting (T_m) and Melting Enthalpy (ΔH_m), Obtained from the First Heating Run and Glass Transition Temperature (T_{g2}), Obtained from the Second Heating Run for Pure and Hybrid PHBV Electrospun Fibers

	T_m (°C)	ΔH_m (J/g)	T_{g2} (°C)
PHBV3	179.4 ± 0.2	92.5 ± 7.2	-
PHBV3 + 15% BCNW	176.2 ± 1.4	89.0 ± 6.7	-
PHBV9	156.5 ± 2.2	50.1 ± 1.4	0.6 ± 1.9
PHBV9 + 15% BCNW	152.6 ± 0.1	52.9 ± 4.5	−1.2 ± 0.7
PHBV16	156.1 ± 2.0	43.5 ± 7.8	1.5 ± 0.6
PHBV16 + 15% BCNW	153.6 ± 0.8	43.4 ± 14.1	1.5 ± 0.6

Characterization of PHBV–BCNW Nanocomposites

Master-batches consisting of the hybrid PHBV–BCNW fibers were subsequently melt mixed with PHBV and nanocomposite films were prepared by compression molding. This strategy was also compared to the conventional process of melt mixing the polymer with the freeze-dried BCNW. The electrospinning pre-incorporation procedure has been proven to be an efficient strategy to enhance the dispersion of BCNW into several matrices such as EVOH[18] and PLA.[20] In this case, the more hydrophobic character of the PHBVs used in this work was expected to further complicate the dispersion of the highly hydrophilic BCNW.

Morphological Characterization. Figure 4 shows the contact transparency images of the different PHBV grades films and of their nanocomposites containing BCNW. As observed, all the materials presented a relatively good contact transparency,

Table III. TGA Maximum of the Weight Loss First Derivate (T_D) and the Corresponding Peak Onset Values and the Residue at 400 and 600°C for Pure and Hybrid PHBV Electrospun Fibers

	Onset T (°C)	T_{D1} (°C)	T_{D2} (°C)	Residue at 400°C (%)	Residue at 600°C (%)
PHBV3	222.9	270.4	-	9.4	8.3
PHBV3 + 15% BCNW	227.8	269.4	345.6	1.3	0.0
PHBV9	223.5	276.9	-	11.5	0.0
PHBV9 + 15% BCNW	225.0	294.1	306.2	5.5	4.3
PHBV16	242.9	287.9	-	7.6	4.7
PHBV16 + 15% BCNW	250.4	290.1	334.7	8.1	5.8

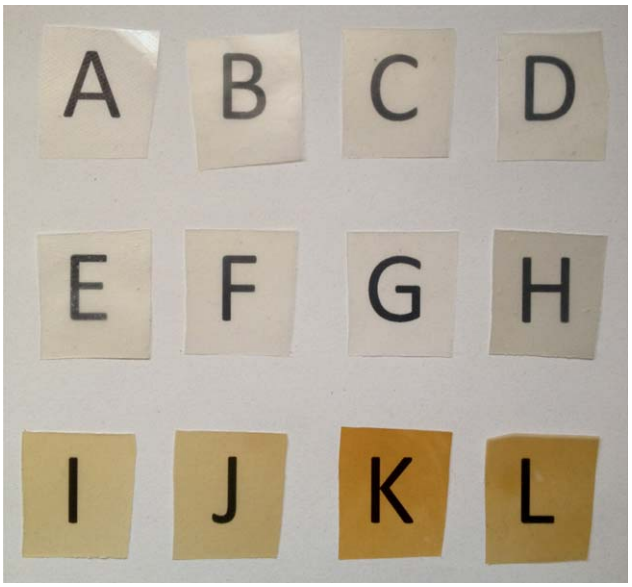

Figure 4. Contact transparency pictures of melt compounded PHBV films: (a) PHBV3; (b) PHBV3 + 1% BCNW ES, (c) PHBV3 + 3% BCNW ES; (d) PHBV3 + 1% BCNW FD; (e) PHBV3 + 3% BCNW FD; (f) PHBV3–PEG; (g) PHBV3–PEG + 1% BCNW ES; (h) PHBV3–PEG + 3% BCNW ES; (i) PHBV9; (j) PHBV9 + 1% BCNW ES; (k) PHBV16; and (l) PHBV16 + 1% BCNW ES. [Color figure can be viewed in the online issue, which is available at wileyonlinelibrary.com.]

which was not compromised by the addition of BCNW. However, some agglomerates could be visually identified for the PHBV3 films incorporating freeze-dried BCNW, indicating a high level of nanofiller aggregation. It is worth noting that when increasing the hydroxyvalerate content, the materials presented slightly higher contact transparency. This fact was also reported for cast PHBV films and it was explained by the presumably lower crystallinity of the higher hydroxyvalerate PHBVs.[16] On the other hand, the higher the hydroxyvalerate content, the more intense the yellowish color of the films. This coloration may be indicative of a certain degree of thermal degradation. This is not consistent with the TGA profiles of the electrospun fibers (cf. Table III) and with the thermal stability reported for various PHBV grades,[16,33] which showed no relationship between the hydroxyvalerate content and the thermostability. However, these TGA analyses did not simulate the actual melt processing conditions as they were developed under N_2 atmosphere. In fact, another work pointed out the fact that higher hydroxyvalerate content PHBVs underwent hydrolytic degradation to a higher extent.[36] It was hypothesized that water molecules entered the amorphous hydroxyvalerate regions to cleave the ester bonds and lead to chain scission of polyester units. Thus, it would be reasonable to hypothesize that the higher hydroxyvalerate PHBVs suffered thermal degradation to a certain extent due to the presence of moisture while they were processed.

To examine the morphology of the neat matrices and of the nanocomposite PHBV films as well as the BCNW dispersion, the cryofractured surfaces of the produced films were examined by SEM and representative images are displayed in Figure 5. When comparing the different polymeric matrices, it was observed that PHBV9, PHBV16, and PHBV3 plasticized with PEG presented a rough surface, whereas the PHBV3 film showed a smoother surface with some cavities which were indicative of the higher brittleness of this material (cf. Table IV).

It is clearly observed that a great level of agglomeration was attained by mixing the freeze-dried BCNW with the PHBV3 [cf. Figure 5(d,e)]. The appearance of these large aggregates is indicative of the particularly low compatibility between the extremely hydrophilic BCNW and the hydrophobic PHBV. The pre-incorporation through electrospinning significantly improved the dispersion of the nanofiller, especially for a low loading such as 1 wt % BCNW. On the other hand, for the plasticized PHBV3, a certain phase separation between the hydrophilic PEG–BCNW domains and the hydrophobic polymer took place, leading to the creation of large voids along the cryofractured surface.

In conclusion, the electrospinning pre-incorporation method allowed loading highly dispersed BCNW into several PHBV grades, although this level of dispersion was slightly lower than that previously achieved for a PLA matrix[20] probably due to higher hydrophobicity of PHBV.

Thermal Properties. Thermal properties of the different PHBV grades and their nanocomposite films were investigated by DSC analyses and the main estimated parameters are gathered in Table V. The pure PHBVs presented a two-step melting behavior, consisting of a sharp melting peak followed by a melting shoulder. The appearance of two melting peaks has been reported for several PHBV grades and it has been attributed to several factors. While some studies hypothesized that more defective or smaller crystals are able to re-crystallize after melting, forming more perfect crystals which subsequently melt at higher temperatures,[13] other works pointed out to the existence of different crystalline phases (HB-rich and HV-rich domains associated to the high- and low-temperature melting processes, respectively).[37] In this work, the ratios of the melting enthalpies corresponding to each peak were clearly not related to the HV content of the samples. Thus, the first hypothesis, implying that a small amount of crystals were able to re-crystallize into a more perfect phase, seemed more feasible. Increasing the HV content from 3 to 9–16 mol % gave rise to lower melting and glass transition temperatures, as well as reduced overall melting enthalpy. The reduced enthalpy might be related to a crystallinity reduction caused by the higher hydroxyvalerate content, but it might also be a consequence of the slight hydrolytic degradation suffered by the higher valerate PHBVs. On the other hand, the incorporation of PEG into the PHBV3 did not reduce the overall crystallinity of the material, but prevented the creation of more perfect crystals after the first melting process, thus showing only one melting peak.

The incorporation of BCNW led to a drop in the melting temperature of both the first and second melting peaks. Additionally, the overall melting enthalpy was reduced only for those samples in which the nanofiller dispersion was very high, i.e., the samples incorporating 1 wt % BCNW through electrospinning. This

behavior was also reported for PHBV8 composites incorporating bamboo pulp fibers by melt compounding[38] and is likely due to the cellulose nanofillers acting as obstacles for the crystallization of PHBV under the rapid cooling conditions applied after melt compounding. Additionally, the glass transition temperature (T_g) of PHBV3 increased with the incorporation of BCNW. This effect has been previously related to a reduced mobility of the PHBV molecular chains in the presence of dispersed cellulose nanocrystals.[12,15] Conversely, the addition of BCNW did not seem to have a significant effect on the T_g values of the PHBV9 and PHBV16 matrices, which may be indicative of weaker matrix–filler interactions, despite the relatively homogeneous dispersion of BCNW observed by SEM. This distinct behavior is likely to be related to the presence of a certain amount of hydrophilic impurities in these two latter PHBV grades. Although the materials were subjected to a purification step which prevented thermal degradation during melt processing, they presented a marked decrease in the T_g as compared

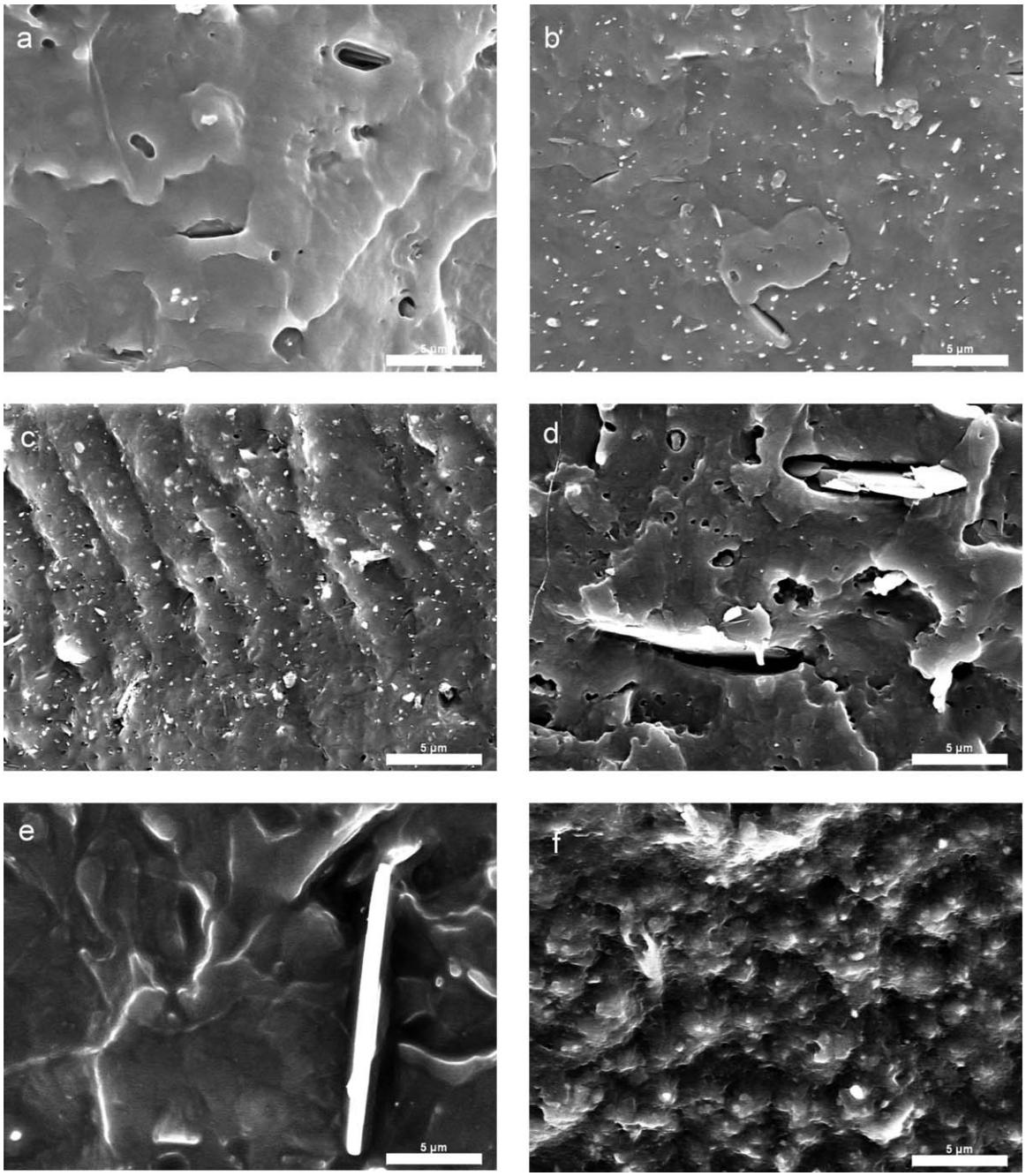

Figure 5. SEM micrographs of cryofractured sections of melt compounded PHBV films: (a) PHBV3; (b) PHBV3 + 1% BCNW ES; (c) PHBV3 + 3% BCNW ES; (d) PHBV3 + 1% BCNW FD; (e) PHBV3 + 3% BCNW FD; (f) PHBV3–PEG; (g) PHBV3–PEG + 1% BCNW ES; (h) PHBV3–PEG + 3% BCNW ES; (i) PHBV9; (j) PHBV9 + 1% BCNW ES; (k) PHBV16; and (l) PHBV16 + 1% BCNW ES.

with the commercial PHBV3. In fact, T_g values typically reported for non-purified PHBV grades are even lower (−2.4 and −4.9°C for PHBV19[11] and −2.7°C for PHBV7[16]), hence confirming that the amount of impurities remaining in the material has a strong impact in the corresponding T_g. If some impurities remain in the material, the BCNW are expected to interact preferentially with these due to their strong hydrophilic behavior, creating separate domains and thus, hindering the interaction between the nanofiller and the hydrophobic PHBV matrix. This hypothesis of weaker BCNW–PHBV interactions for the PHBV9 and PHBV16 is further supported by the barrier and mechanical properties described in the following sections.

Mechanical Properties. Table IV summarizes the mechanical properties of the neat PHBV matrices and of their nanocomposites. From these results, it may be deduced that the mechanical properties were affected by both the hydroxyvalerate content of the PHBV and the presence of plasticizer, whereas the incorporation of low loadings of BCNW did not lead to significant changes.

Considering the data corresponding to the different PHBV grades, the greater ductility of the high hydroxyvalerate PHBVs was evidenced by their significantly reduced Young's modulus and increased elongation at break. This observation is in

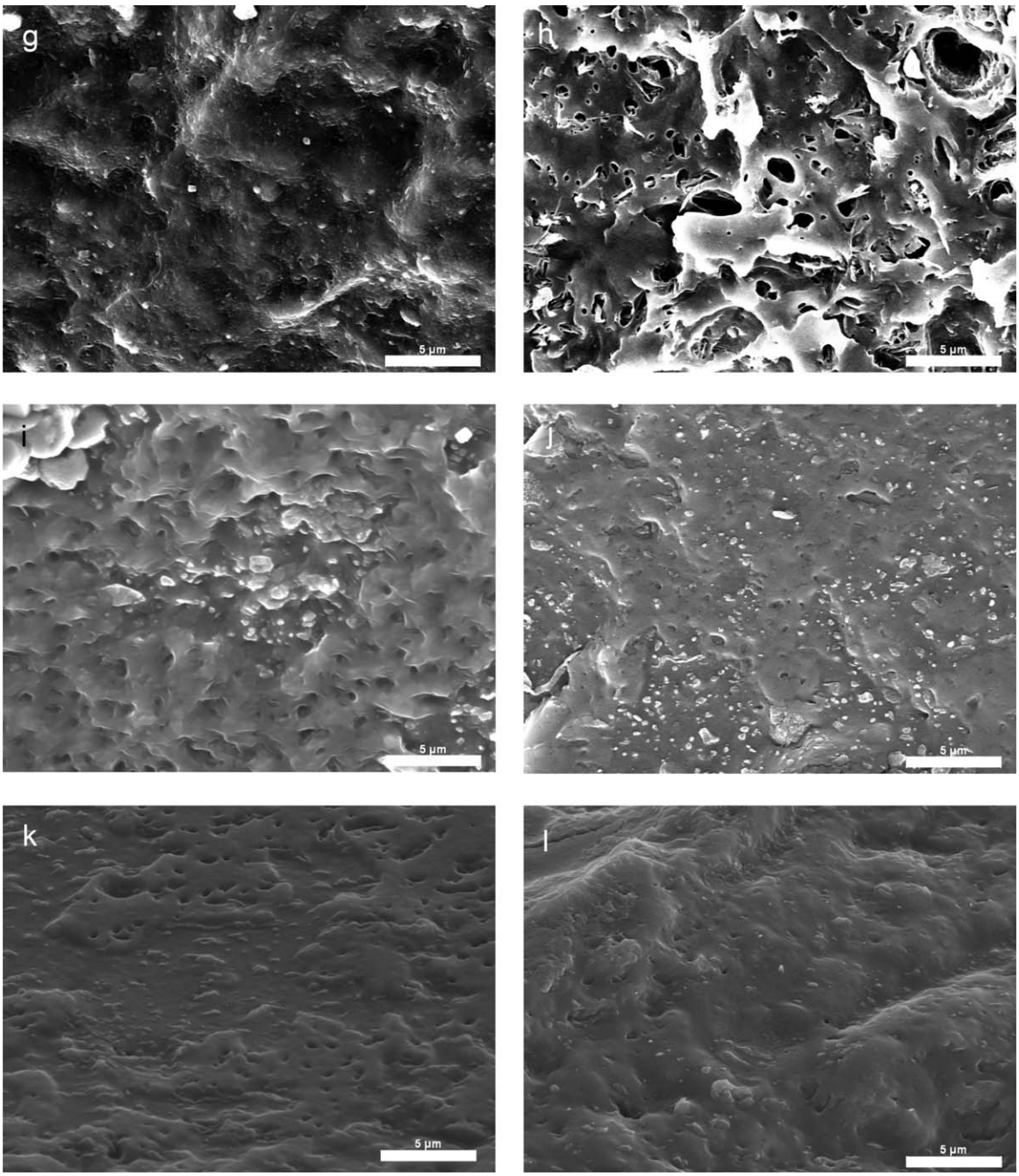

Figure 5. (*Continued*)

Table IV. Young's Modulus, Tensile Strength, and Elongation at Break of Melt Compounded PHBV Films and Their Nanocomposites with BCNW

	E (GPa)	Tensile strength (MPa)	ε_b (%)
PHBV3	2.32 ± 0.12^{c}	30.67 ± 1.24^{cd}	1.90 ± 0.10^{a}
PHBV3 + 1% BCNW ES	2.00 ± 0.18^{c}	22.69 ± 4.18^{ab}	2.20 ± 0.22^{abc}
PHBV3 + 3% BCNW ES	2.30 ± 0.26^{c}	28.90 ± 4.22^{bcd}	1.88 ± 0.14^{a}
PHBV3 + 1% BCNW FD	2.30 ± 0.27^{c}	32.17 ± 4.20^{de}	2.15 ± 0.30^{abc}
PHBV3 + 3% BCNW FD	2.11 ± 0.20^{c}	28.90 ± 3.35^{bcd}	2.00 ± 0.48^{ab}
PHBV3-PEG	2.21 ± 0.24^{c}	38.80 ± 6.13^{e}	3.10 ± 0.57^{de}
PHBV3-PEG + 1% BCNW ES	1.51 ± 0.15^{b}	23.94 ± 3.46^{abc}	2.89 ± 0.18^{cde}
PHBV3-PEG + 3% BCNW ES	1.41 ± 0.20^{ab}	18.40 ± 3.57^{a}	2.38 ± 0.29^{abcd}
PHBV9	1.13 ± 0.02^{ab}	26.71 ± 1.97^{bcd}	3.35 ± 0.42^{e}
PHBV9 + 1% BCNW ES	1.09 ± 0.06^{a}	22.89 ± 2.47^{ab}	2.71 ± 0.57^{bcde}
PHBV16	1.38 ± 0.05^{ab}	30.19 ± 3.03^{bcd}	3.11 ± 0.44^{de}
PHBV16 + 1% BCNW ES	1.47 ± 0.12^{ab}	29.36 ± 2.49^{bcd}	2.78 ± 0.13^{bcde}

The a, b, c, d, and e letters correspond to the ANOVA statistical analysis and Turkey test of the data that indicate that with a 95% confidence level, the values are significantly different.

agreement with previous works[16,26,33] and it suggests that somehow the presence of hydroxyvalerate groups increased the mobility of the molecular PHBV chains.

PHBV3 presented an excellent rigidity and strength but and excessive brittleness. To enhance its mechanical performance, 5 wt % of PEG was incorporated into PHBV3, giving rise to a significantly increased elongation at break and tensile strength, without affecting the Young's modulus. The same ductility increase was observed for PHB films plasticized with PEG prepared by casting, although in that case, the tensile strength was diminished, probably as a result of the high amount of plasticizer (15 wt % PEG).[39]

The mechanical performance of PHBVs was not altered by the incorporation of BCNW. Only the plasticized PHBV3 showed reduced Young's modulus, tensile strength, and elongation at break with the addition of BCNW. This behavior may be indicative of a certain phase separation between the hydrophilic PEG–BCNW domains and the hydrophobic PHBV, as commented on above.

A recent work in which nanofibrillated cellulose was incorporated into PHBV by melt compounding, reported a significant embrittlement effect caused by agglomeration of the nanofiller and by the nanocomposite degradation, favored by the presence of cellulose.[17] This effect was not evident for the materials developed in this work, as no significant nanofiller agglomeration was observed with the electrospinning pre-incorporation method and no thermal degradation seemed to be triggered by the presence of the filler. On the other hand, the lack of mechanical improvement in the nanocomposites differs from several studies in which highly dispersed BCNW presented a significant stiffening effect on PLA and EVOH melt compounded nanocomposites.[19,20] Also in contrast with these studies, no differences in the mechanical properties were found

Table V. DSC Maximum of Melting (T_{m1} and T_{m2}) and Melting Enthalpy (ΔH_{m1} and ΔH_{m2}), Obtained from the First Heating Run and Glass Transition Temperature (T_{g2}), Obtained from the Second Heating Run

	T_{m1} (°C)	ΔH_{m1} (J/g)	T_{m2} (°C)	ΔH_{m2} (J/g)	T_{g2} (°C)
PHBV3	171.0 ± 0.6	75.9 ± 0.4	184.7 ± 0.9	4.6 ± 0.3	3.0 ± 1.0
PHBV3 + 1% BCNW ES	162.5 ± 0.0	25.2 ± 2.9	171.4 ± 0.5	26.4 ± 0.4	5.7 ± 0.7
PHBV3 + 3% BCNW ES	169.2 ± 0.7	78.3 ± 4.3	184.3 ± 0.8	3.1 ± 0.8	5.2 ± 0.5
PHBV3 + 1% BCNW FD	169.5 ± 0.0	78.5 ± 0.4	-	-	5.1 ± 0.0
PHBV3 + 3% BCNW FD	169.2 ± 1.2	74.1 ± 8.6	-	-	5.2 ± 0.3
PHBV3-PEG	171.0 ± 1.1	89.4 ± 6.5	-	-	-
PHBV3-PEG + 1% BCNW ES	170.4 ± 0.0	90.0 ± 1.1	-	-	-4.4 ± 0.8
PHBV3-PEG + 3% BCNW ES	169.2 ± 0.0	86.7 ± 1.0	-	-	-5.8 ± 1.7
PHBV9	143.5 ± 0.4	27.6 ± 7.0	164.6 ± 0.2	7.7 ± 1.0	-0.1 ± 0.1
PHBV9 + 1% BCNW ES	139.6 ± 1.1	5.1 ± 0.2	155.3 ± 0.4	14.5 ± 1.1	1.1 ± 0.7
PHBV16	149.0 ± 0.5	29.3 ± 0.5	170.4 ± 0.0	5.5 ± 0.1	0.5 ± 0.2
PHBV16 + 1% BCNW ES	145.0 ± 0.7	22.3 ± 0.7	167.0 ± 0.0	10.1 ± 1.3	-0.1 ± 0.1

Table VI. Water Permeability Measured at 85% Relative Humidity and Oxygen Permeability Measured at 80% Relative Humidity of Melt Compounded PHBV Films and Their Nanocomposites with BCNW

	PH_2O 85% RH (Kg·m/s·m^2·Pa)	PO_2 80% RH(m^3·m/ m^2·s·Pa)
PHBV3	$0.59 \pm 0.06\ e^{-15a}$	$1.56 \pm 0.27\ e^{-19bc}$
PHBV3 + 1% BCNW ES	$1.03 \pm 0.03\ e^{-15a}$	$0.93 \pm 0.01\ e^{-19a}$
PHBV3 + 3% BCNW ES	$1.02 \pm 0.02\ e^{-15a}$	$1.12 \pm 0.07\ e^{-19b}$
PHBV3 + 1% BCNW FD	$1.13 \pm 0.04\ e^{-15ab}$	$1.64 \pm 0.22\ e^{-19bc}$
PHBV3 + 3% BCNW FD	$3.49 \pm 1.34\ e^{-15cd}$	$3.09 \pm 0.10\ e^{-19de}$
PHBV3-PEG	$4.62 \pm 0.16\ e^{-15d}$	$2.55 \pm 0.22\ e^{-19cd}$
PHBV3-PEG + 1% BCNW ES	$2.82 \pm 0.03\ e^{-15bc}$	$3.42 \pm 0.73\ e^{-19de}$
PHBV3-PEG + 3% BCNW ES	$4.69 \pm 0.71\ e^{-15d}$	$4.26 \pm 0.31\ e^{-19de}$
PHBV9	$0.85 \pm 0.10\ e^{-15a}$	$3.13 \pm 0.10\ e^{-19de}$
PHBV9 + 1% BCNW ES	$0.73 \pm 0.04\ e^{-15a}$	$3.61 \pm 0.03\ e^{-19de}$
PHBV16	$2.22 \pm 0.14\ e^{-15abc}$	$4.13 \pm 0.42\ e^{-19e}$
PHBV16 + 1% BCNW ES	$3.84 \pm 0.24\ e^{-15cd}$	$5.40 \pm 0.23\ e^{-19f}$

The a, b, c, d, e, and f letters correspond to the ANOVA statistical analysis and Turkey test of the data that indicate that with a 95% confidence level, the values are significantly different.

when comparing the direct melt mixing of freeze-dried BCNW (which resulted in large agglomerates) and the electrospinning pre-incorporation. This may indicate that in the case of PHBV, it was the weak matrix–filler interactions that were mostly influencing the mechanical performance rather than the level of BCNW dispersion.

Water and Oxygen Barrier Properties. The barrier properties of the PHBVs and their nanocomposites were evaluated by measuring the water and oxygen permeability at high relative humidity, to approach the conditions found in real food packaging systems. The results gathered in Table VI evidence that the hydroxyvalerate content, the presence of plasticizer, and the addition of BCNW considerably affected the barrier performance of PHBVs.

In general, there was a trend of increased water and oxygen permeability when increasing the hydroxyvalerate content in the PHBV matrix, which may be related to the crystallinity decrease observed for the high hydroxyvalerate PHBVs.[16,33,40]

The incorporation of PEG as plasticizer led to a significant barrier decrease, being this effect more evident for the water barrier. This behavior was also observed for melt compounded PLA plasticized with PEG and it was mainly attributed to an increased free volume as a consequence of the higher mobility of PHBV chains.[41] PEG is also known to contain OH groups, which may increase the solubility of water molecules into the films, having a negative impact on the water barrier performance.

Regarding the incorporation of BCNW, some improvements in the barrier performance of PHBVs were observed. Due to their highly hydrophilic character of the filler, the water permeability was expected to increase with the addition of BCNW. This was certainly the case when freeze-dried BCNW were melt mixed with PHBV3, promoting water diffusion through preferential paths created as a result of the nanofiller agglomeration. However, this negative effect was limited by the good dispersion and distribution achieved with the electrospinning pre-incorporation method. It was even possible to reduce the water permeability of the PHBV3–PEG sample by incorporating 1 wt % BCNW (*ca* 39% water permeability drop). Even though phase separation probably took place in the PEG plasticized samples, the reduction of OH groups available for water sorption as a result of the interactions established between PEG and BCNW could be responsible for the reduced permeability at low nanofiller loadings.

Regarding the oxygen permeability, the trend was similar to that observed for the water barrier. Whereas the oxygen barrier was significantly reduced with the agglomeration of freeze-dried BCNW, improvements were detected with the addition of highly dispersed BCNW (with *ca* 40% oxygen permeability drop for the PHBV3 loaded with 1 wt % BCNW). This again highlights the efficiency of the electrospinning pre-incorporation method, providing high nanofiller dispersion despite the low PHBV–BCNW compatibility.

It should also be considered that the blocking capacity of BCNW was strongly limited by the high relative humidity conditions used to perform the measurements. The barrier performance of BCNW has been shown to be especially sensitive to moisture and previous studies on PLA and PHBV matrices showed that BCNW were able to greatly reduce the oxygen permeability at low relative humidity, the addition of BCNW should be restricted to low loadings to preserve or slightly improve the barrier properties of the matrices with the presence of moisture.[16,20]

Although several works reported on the production of PHBV nanocomposites loaded with CNW,[13–15,17] no attention has been drawn to their effect on mass transport properties. We have formerly evaluated the barrier properties of PHBV films containing BCNW developed by solution casting.[16] As compared with the previous work, this study represents a considerable advance as it

provides an efficient and industrially applicable method for the production of PHBV–BCNW nanocomposites, with permeability reductions even higher than those reported for the cast films.

CONCLUSIONS

Bacterial nanocomposites with improved barrier properties were produced by melt compounding using PHBVs as polymeric matrices and BCNW as nanofillers. Two PHBV grades (PHBV9 and PHBV16) were synthesized by microbial mixed cultures using food industry waste feedstocks and compared to a commercial grade (PHBV3). Both the plasticization with PEG and increasing the hydroxyvalerate content were favorable in terms of mechanical performance as the ductility was increased but, on the other hand, they gave rise to a decrease in the barrier properties.

The incorporation of BCNW was investigated in order to improve the properties of the PHBV matrices. Due to the extremely low compatibility between the hydrophobic PHBV and the highly hydrophilic BCNW, the conventional process of melt mixing the polymer with the freeze-dried BCNW resulted in large agglomerates and phase separation. This negative effect was completely avoided by using a method based on the pre-incorporation of BCNW by electrospinning to form a masterbatch that can be later melt blended with virgin resin.

The relatively weak matrix–filler interactions most likely impeded the reinforcing effect of BCNW even when highly dispersed and, thus, the mechanical properties of PHBVs were not significantly affected by the presence of the nanofiller. On the other hand, a high dispersion was seen to be critical in order to preserve or slightly improve the barrier properties. Thus, whereas the addition of freeze-dried BCNW was detrimental due to the creation of preferential diffusion paths, this was not the case when BCNW were incorporated through electrospinning. Even though the extremely high moisture sensitivity of BCNW most likely impaired their blocking effect at high relative humidity conditions, i.e., in the application conditions, it was possible to significantly reduce the oxygen permeability of PHBV3 with a 1 wt % BCNW loading.

This work has demonstrated that the electrospinning pre-incorporation method, in here termed as the electrospinning enabling melt compounding route, is an efficient strategy to guarantee a high dispersion of BCNW even in highly hydrophobic matrices such as PHBVs by melt compounding, providing materials suitable for high barrier food packaging applications. In addition, more economically viable route such as the synthesis by microbial mixed cultures with no-cost waste feedstocks can be used to produce PHBVs, although in the future, lower hydroxyvalerate PHBVs should be targeted as they will provide for a start enhanced barrier performance.

ACKNOWLEDGMENTS

M. Martínez-Sanz would like to thank the Spanish Ministry of Education for the FPU grant. A. Lopez-Rubio is the recipient of a "Ramon y Cajal" contract from the Spanish Ministry of Science and Innovation. C. S. S. Oliveira acknowledges FCT for the grant SFRH/BPD/88817/2012. M. Villano and M. Majone would like to thank Sabrina Campanari (Sapienza University of Rome) for the skilful assistance with the experimental work. The authors acknowledge financial support from the EU FP7 ECOBIOCAP and MAT2012- 38947-C02-01 projects. The Electronic Microscopy department in the SCIE from the University of Valencia is acknowledged for the support with SEM and TEM analyses. Dr. Luis Cabedo, from Universitat Jaume I, is acknowledged for his support with mechanical testing.

REFERENCES

1. Lundgren, D. G.; Alper, R.; Schnaitman, C.; Marchessault, R. H. *J. Bacteriol.* **1965**, *89*, 245.
2. Barham, P. J.; Keller, A.; Otun, E. L.; Holmes, P. A. *J. Mat. Sci.* **1984**, *19*, 2781.
3. Scandola, M.; Ceccorulli, G.; Pizzoli, M.; Gazzano, M. *Macromolecules* **1992**, *25*, 1405.
4. Serafim, L. S.; Lemos, P. C.; Torres, C.; Reis, M. A. M.; Ramos, A. M. *Macro. Biosci.* **2008**, *8*, 355.
5. Wang, Y.; Yamada, S.; Asakawa, N.; Yamane, T.; Yoshie, N.; Inoue, Y. *Biomacromolecules* **2001**, *2*, 1315.
6. Chen, L. J.; Wang, M. *Biomaterials* **2002**, *23*, 2631.
7. Feng, L.; Watanabe, T.; Wang, Y.; Kichise, T.; Fukuchi, T.; Chen, G. Q.; Doi, Y.; Inoue, Y. *Biomacromolecules* **2002**, *3*, 1071.
8. Drieskens, M.; Peeters, R.; Mullens, J.; Franco, D.; Iemstra, P. J.; Hristova-Bogaerds, D. G. *J. Polym. Sci., Part B: Polym. Phys.* **2009**, *47*, 2247.
9. Choi, J. I.; Lee, S. Y. *Bioprocess. Eng.* **1997**, *17*, 335.
10. Reis, M. A. M.; Albuquerque, M. G. E.; Villano, M.; Majone, M. In *Comprehensive Biotechnology*; A. S. Fava F, Young M, Eds.; Elsevier: **2011**, p 669.
11. Duque, A. F.; Oliveira, C. S. S.; Carmo, I. T. D.; Gouveia, A. R.; Pardelha, F.; Ramos, A. M.; Reis, M. A. M. *New Biotechnology* **2014**, *31*, 276.
12. Ten, E.; Bahr, D. F.; Li, B.; Jiang, L.; Wolcott, M. P. *Ind. Eng. Chem. Res.* **2012**, *51*, 2941.
13. Ten, E.; Turtle, J.; Bahr, D.; Jiang, L.; Wolcott, M. *Polymer* **2010**, *51*, 2652.
14. Yu, H. Y.; Qin, Z. Y.; Liu, Y. N.; Chen, L.; Liu, N.; Zhou, Z. *Carbohydr. Polym.* **2012**, *89*, 971.
15. Jiang, L.; Morelius, E.; Zhang, J.; Wolcott, M.; Holbery, J. *J. Compos. Mater.* **2008**, *42*, 2629.
16. Martínez-Sanz, M.; Villano, M.; Oliveira, C.; Albuquerque, M. G. E.; Majone, M.; Reis, M. A. M.; Lopez-Rubio, A.; Lagaron, J. *New Biotechnology* **2014**, *31*, 364.
17. Srithep, Y.; Ellingham, T.; Peng, J.; Sabo, R.; Clemons, C.; Turng, L. S.; Pilla, S. *Polym. Degrad. Stab.* **2013**, *98*, 1439.
18. Martínez-Sanz, M.; Lopez-Rubio, A.; Lagaron, J. M. *J. Appl. Polym. Sci.* **2013**, *128*, 2666.
19. Martínez-Sanz, M.; Lopez-Rubio, A.; Lagaron, J. M. *J. Appl. Polym. Sci.* **2013**, *128*, 2197.

20. Martínez-Sanz, M.; Lopez-Rubio, A.; Lagaron, J. M. *Biomacromolecules* **2012**, *13*, 3887.
21. Martínez-Sanz, M.; Olsson, R. T.; Lopez-Rubio, A.; Lagaron, J. M. *Cellulose* **2011**, *18*, 335.
22. Martínez-Sanz, M.; Lopez-Rubio, A.; Lagaron, J. M. *Carbohydr. Polym.* **2011**, *85*, 228.
23. Scoma, A.; Bertin, L.; Zanaroli, G.; Fraraccio, S.; Fava, F. *Bioresour. Technol.* **2011**, *102*, 10273.
24. Villano, M.; Valentino, F.; Barbetta, A.; Martino, L.; Scandola, M.; Majone, M. *New Biotechnology* **2014**, *31*, 289.
25. Serafim, L. S.; Lemos, P. C.; Oliveira, R.; Reis, M. A. M. *Biotechnol. Bioeng.* **2004**, *87*, 145.
26. Savenkova, L.; Gercberga, Z.; Bibers, I.; Kalnin, M. *Process Biochem.* **2000**, *36*, 445.
27. Madden, L. A.; Anderson, A. J.; Asrar, J. *Macromolecules* **1998**, *31*, 5660.
28. Suwantong, O.; Waleetorncheepsawat, S.; Sanchavanakit, N.; Pavasant, P.; Cheepsunthorn, P.; Bunaprasert, T.; Supaphol, P. *Int. J. Biol. Macromol.* **2007**, *40*, 217.
29. Yoon, Y. I.; Moon, H. S.; Lyoo, W. S.; Lee, T. S.; Park, W. H. *J. Colloid Interface Sci.* **2008**, *320*, 91.
30. Sombatmankhong, K.; Suwantong, O.; Waleetorncheepsawat, S.; Supaphol, P. *J. Polym. Sci., Part B: Polym. Phys.* **2006**, *44*, 2923.
31. Martínez-Sanz, M.; Lopez-Rubio, A.; Lagaron, J. M. *J. Polym. Environ.* **2014**, *22*, 27.
32. Chen, L.; Zhu, M.; Song, L.; Yu, H.; Zhang, Y.; Chen, Y.; Adler, H. J. *Macromol. Symp.* **2004**, *210*, 241.
33. Modi, S.; Koelling, K.; Vodovotz, Y. *Eur. Polym. J.* **2011**, *47*, 179.
34. Martínez-Sanz, M.; . Bilbao-Sainz, C.; Du, W. X.; Chiou, B. S.; Williams, T. G.; Wood, D. F.; Imam, S. H.; Orts, W. J.; Lopez-Rubio, A.; Lagaron, J. M. *J. Nanoscience and Nanotechnology* **2015**, *15*, 616.
35. Liu, D.; Xiaowen, X.; Bhattacharyya, D. *J. Mater. Sci. Lett.* **2012**, *47*, 3159.
36. Liu, H.; Pancholi, M.; Stubbs Iii, J.; Raghavan, D. *J. Appl. Polym. Sci.* **2010**, *116*, 3225.
37. Arcos-Hernández, M. V.; Laycock, B.; Donose, B. C.; Pratt, S.; Halley, P.; Al-Luaibi, S.; Werker, A.; Lant, P. A. *Eur. Polym. J.* **2013**, *49*, 904.
38. Jiang, L.; Huang, J.; Qian, J.; Chen, F.; Zhang, J.; Wolcott, M. P.; Zhu, Y. *J. Polym. Environ.* **2008**, *16*, 83.
39. Rahman, M. A.; De Santis, D.; Spagnoli, G.; Ramorino, G.; Penco, M.; Phuong, V. T.; Lazzeri, A. *J. Appl. Polym. Sci.* **2013**, *129*, 202.
40. Shogren, R. *Journal of Environmental Polymer Degradation* **1997**, *5*, 91.
41. Courgneau, C.; Domenek, S.; Guinault, A.; Avérous, L.; Ducruet, V. *J. Polym. Environ.* **2011**, *19*, 362.